

Original Article

circ_JMJD1C expedites breast cancer progression by regulating miR-182-5p/JMJD1C/SOX4 axis

Renyuan Xu, Haomiao Lan, Li Zhang, Sisi Yang, Yu Mao, Hongying Che*

Department of Thyroid and Breast Surgery, Zigong First People's Hospital, Zigong 643000, Sichuan, China

Article Info

Abstract



Article history:

Received: November 10, 2023

Accepted: February 21, 2024

Published: March 31, 2024

Use your device to scan and read the article online



Circular RNAs (circRNAs) are engaged in various types of cancers. This study aimed to investigate the roles of circ_0006743 (circ_JMJD1C) in breast cancer. The downstream of circ_JMJD1C and their interaction network was determined by bioinformatic analyses. Gene expression were analyzed through western blot and qRT-PCR assays. Functional assays were conducted in vitro and in vivo to verify circ_JMJD1C role in BC. FISH and confocal analysis indicated the cellular distribution of circ_JMJD1C. Luciferase reporter, RNA immune-precipitation (RIP) assays, as well as Pearson's correlation analysis, were implemented to test the relation of miR-182-5p, JMJD1C and circ_JMJD1C. Circ_JMJD1C and JMJD1C expression were both elevated, and their expression was positively correlated in BC. Circ_JMJD1C knockdown hindered BC cell proliferation, invasion, and migration, along with epithelial-mesenchymal transition (EMT) in vitro and in vivo. Circ_JMJD1C facilitated BC progression by the miR-182-5p-JMJD1C axis. Circ_JMJD1C epigenetically upregulated SOX4. Circ_JMJD1C promotes the aggressiveness of BC via regulating miR-182-5p/JMJD1C/SOX4 axis. This may provide a novel and promising therapy targeting BC.

Keywords: Breast cancer; hsa_circ_0006743; miR-182-5p; JMJD1C.

1. Introduction

Breast cancer (BC) belongs to a recurrent malignancy, as well as is a major cause of cancer-linked mortality in females all over the world [1, 2]. Despite varying degrees of improvement in diagnosis, prognosis, and treatment, the recurrence together with mortality rates in women with BC remains high [3, 4]. Thus, efficient diagnostic or therapeutic approaches are required to understand and identify vital molecular targets engaged in the progression of BC.

Circular RNAs (circRNAs) belong to a novel category of non-coding RNAs that generate a connecting loop at 3' and 5' ends [5]. Since circRNA is widely expressed in mammals [6], its potential role in human diseases has shed light on researching their mechanism [7]. Recently, numerous literatures have probed the potential of different novel circRNAs in BC [8]. For example, circRNA_0025202 affects BC progression through the miR-182-5p-FOXO3a axis [9]. CircCDYL regulates the miR-1275-ATG7/ULK1-autophagic axis to facilitate BC progression [10]. CircRNF20 increases BC tumorigenesis as well as the Warburg effect via miR-487a-HIF-1 α -HK2 [11]. However, the identification of novel circRNAs associated with BC pathogenesis and progression is important to maximize therapeutic efficiency.

Herein, the potential of a novel circRNA hsa_

circ_0006743 (circ_JMJD1C) in BC progression was probed. Circ_JMJD1C has been registered to be upregulated in BC and contributed to BC progression [12]. Circ_JMJD1C is derived from its host gene Jumonji Domain Containing 1C (JMJD1C), which is located in 10q21.3, and it is suggested to possess an oncogenic role in BC [12]. Accumulating reports have elucidated the vital role of JMJD1C in cancer [13]. Intriguingly, a similar circRNA, circ-TFF1, has been reported to positively regulate its host gene TFF1 in BC by competitively combining with miR-326 [14]. This phenomenon has relied on their closely related location in the human genome. Our findings utilized a similar hypothesis and investigated the role of circ_JMJD1C and its relation to JMJD1C in BC progression. We proved that circ_JMJD1C/miR-182-5p/JMJD1C axis had a tumor-promoting potential in BC, providing a promising biomarker for the therapy of BC patients in the near future.

2. Materials and methods

2.1. Sample collection

BC tissues (n = 14), para-carcinoma tissues (n = 12), as well as adjacent normal tissues (n = 11), were provided by 14 patients with this cancer in Zigong First People's Hospital. After biopsies or sample resection, all samples

* Corresponding author.

E-mail address: chy1234560526@163.com (H. Che).

Doi: <http://dx.doi.org/10.14715/cmb/2024.70.3.31>

were maintained in tubes supplemented with the RNase inhibitor and stored in liquid nitrogen. All samples were collected after signing an informed consent form. None of the enrolled patients had received any therapy before this study. The present experiments were approved by the ethical committee of Zigong First People's Hospital.

2.2. Cell culture

Procell Life Science & Technology Co., Ltd provided BC cell lines (MCF-7, BT-549, MDA-MB-453, and MDA-MB-231), as well as the normal breast cells (MCF-10A). DMEM (Gibco, USA) supplementing with 10% FBS (Gibco) was implemented for cell culture at 37°C with 5% CO₂.

2.3. Cell transfection

GenePharma (Shanghai, China) provided sh-circ-JMJD1C#1/2/3, miR-182-5p inhibitor, as well as sh-JMJD1C#1 together with the respective controls. Lipofectamine 3000 (Thermo Fisher Scientific, USA) was implemented for cell transfection.

2.4. qRT-PCR

Firstly, total RNA extraction was implemented using TRIzol reagent (Thermo Fisher Scientific), followed by reverse transcription using RevertAid First Strand cDNA Synthesis Kit (Thermo Fisher Scientific). Next, qPCR was determined using SYBR Green PCR Master Mix (Applied Biosystems) and following the 2^{-ΔΔCT} method. Gene expression was normalized to GAPDH or U6.

2.5. Western blot

Total protein from cell or tissue samples was extracted using RIPA buffer (#ab156034, Abcam, Cambridge, UK). A total amount of extracted proteins (20 μg) was electrophoresed in 10% SDS-PAGE and then shifted onto a PVDF membrane (#E-BC-R266, Elabscience). Membranes were sealed in 5% fat-free milk for one hour and followed by incubation with each designated primary antibody, containing anti-Bcl-2 (#ab32124, Abcam), anti-Bax (#ab32503, Abcam), anti-cleaved caspase-3 (#ab32042, Abcam), anti-caspase-3 (#ab32351, Abcam), anti-E-cadherin (#ab40772, Abcam), anti-N-cadherin (#ab76011, Abcam), anti-Fibronectin (#ab2413, Abcam), anti-Vimentin (#ab92547, Abcam), anti-JMJD1C (#ab130922, Abcam), anti-GAPDH (#ab8245, Abcam) overnight at 4°C. Next, membranes were washed thrice and then treated with the corresponding Rabbit Anti-Mouse IgG H&L (HRP) (#ab6721, Abcam). The iBright Analysis Software (Thermo Fisher Scientific) was employed to determine the protein band intensities with GAPDH as an internal control.

2.6 TUNEL assay

The cellular apoptosis rate was determined using the TUNEL assay kit (#E-CK-A322, Elabscience). All treated cells underwent fixation using 4% paraformaldehyde at 4°C. Next, the cells were stained using the TUNEL kit, while the nuclei of cells were stained using DAPI (#ab285390, Abcam), followed by counting using a BX53 fluorescence microscope.

2.7. CCK-8 assay

The cell viability was measured using a Cell Counting

Kit-8 (#ab228554, Abcam) as instructed by the manufacturer. Approximately 2×10³ cells/well were planted into 96-well plates. Each well was treated with CCK-8 solution (10 μL) for 2 hours of incubation. Lastly, The OD values were measured using a microplate reader at 450 nm.

2.8. EdU assay

The proliferation of BC cells was assessed using the EdU assay detection kit (#ab222421, Abcam). 5000 cells/well were planted in 96-well plates. Following forty-eight hours of incubation, the plates were treated with 50 μmol/L EdU labeling media and then incubated for an additional two hours. Next, the cells were treated with 0.5% Triton X-100 and 4% paraformaldehyde then treated with an anti-EdU working solution. DAPI was used to stain the nucleus. The proportion of EdU-positive cells was quantified using a fluorescent microscope. The images were taken from five random fields.

2.9. Transwell assay

Cell invasion assay was conducted using 24-well chambers with 8 μm sized-pores (Sigma-Aldrich). BC cells (5 × 10⁴ cells/well) were cultured in serum-free media and placed in the upper chamber pre-coated with matrigel (Corning). The lower chamber was loaded with a culture medium supplemented with 10% FBS. After 24 h incubation, the upper chambers were removed, and the invasive cells were fixed with methanol and then subjected to staining. At last, the cells were examined and counted under a BX53 microscope at 200× magnification power.

2.10. Wound healing assay

BC cells (5 × 10⁵) were placed in 6-well plates. The wound induction was made via a sterile 200 μL plastic pipette tip to scrap the cell layer. The cells were further supplemented with a culture medium containing 1% FBS and incubated for 36 h. Next, all plates were examined under a BX53 microscope at 50× magnification power.

2.11. Cellular fractionation

The cytoplasm and nucleus of BC cells were separated using a PARIS kit (Thermo Fisher Scientific) in order to segregate the cytoplasmic and nuclear RNA. The concentration of fractionated RNA was assessed using qRT-PCR.

2.12. Fluorescent in-situ hybridization (FISH)

A FISH kit (#F32949, Thermo Fisher Scientific) was utilized for this experiment, and the FISH probes were designed from RIBOBIO (Guangzhou, China). BC cells were fixed in 4% formaldehyde and subsequently dehydrated with ethanol. Next, cells were treated with hybridization buffer mixed with the FISH probes for incubation. After washing and staining using DAPI solution, the cells were examined under a fluorescence microscope (BX63, Olympus, Tokyo, Japan).

2.13. RNA immunoprecipitation (RIP) assay

The AGO2-RIP assay was implemented using EZ-Magna RIP Kit (Sigma-Aldrich). Briefly, the lysates of BC cells were incubated in RIP buffer containing magnetic beads-conjugated human anti-Ago2 or nonspecific mouse IgG antibodies (both from Abcam). Precipitation was conducted using magnets, then the immunoprecipitants were digested by proteinase K, and the released RNAs

were analyzed by qRT-PCR.

2.14. RNA pull-down assay

Briefly, BC cell lysates were incubated with biotin (Bio)-labeled circ-JMJD1C probes (RIBOBIO) at 25°C for two hours. Streptavidin-coupled Dynabeads (#11205D, Thermo Fisher Scientific) were utilized to capture the circ-JMJD1C-linked miRNA complexes. The beads/RNA complexes were incubated for one hour at 25°C in RIPA wash buffer (#R0278, Sigma-Aldrich) containing proteinase K. Successful RNA pull-down was determined using qRT-PCR analysis.

2.15. Luciferase reporter assay

The wild-type or mutated circ-JMJD1C contains miR-182-5p binding sites obtained from Circular RNA Interactome. The constructs were subcloned into the pmirGLO Vector (Promega). Then, miR-182-5p mimic or its control, circ-JMJD1C-WT, circ-JMJD1C-MUT, circ-JMJD1C overexpression plasmids, JMJD1C overexpression plasmids, or the corresponding vectors were co-transfected into BC cells. Twenty-four hours post-transfection, the luciferase activity was evaluated using the Dual-Glo® Luciferase Assay System (Promega).

2.16. ChIP assay

ChIP assay was conducted using a ChIP kit (cat. no. 26157, Thermo Fisher Scientific Inc., USA) according to the manufacturer's protocols. Briefly, cells were fixed in 1% formaldehyde and resuspended in lysis buffer. Then shearing chromatin was performed by adding enzymatic shearing cocktail and stopped by supplementing with EDTA. After pre-cleared with Protein A/G agarose beads, the supernatants were incubated with anti-JMJD1C (3100, 1: 50, CST, USA) or anti-IgG (ab172730, 1: 30, Abcam, USA). The collected chromatin was eluted and proteinase K. ChIP-enriched DNA was determined using PCR.

2.17. Bioinformatics analysis

The binding sites between miR-182-5p and circ-JMJD1C/JMJD1C were analyzed by using the online database Starbase3.0 (<http://starbase.sysu.edu.cn/>). The expression of epithelial-to-mesenchymal transition transcription factors (EMT-TFs), correlation between SOX4 and JMJD1C expression as well as survival rates of breast cancers were analyzed by using the online database GEPIA (<http://gepia.cancer-pku.cn/>).

2.18. Tumor formation and in vivo metastasis assay

Three male BALB/C nude mice (4-6 weeks old) were commercially bought from Nanjing Aibei Biotechnology Co., Ltd. BT-549 cells (1×10^6) harbors sh-NC or sh-circ-JMJD1C plasmids were injected into the posterior side of the mice. Each mice group contained five mice. The xenograft tumor growth was determined every two days. Four weeks later, the mice were sacrificed, and the lungs were harvested. The metastatic nodules were observed via IHC analysis. The present study was conducted and strictly followed up with the requirements of the National Institutes of Health (NIH) for animal experiments and obtained approval from the animal care committee of Zigong First People's Hospital.

2.19. Statistical analysis

The present study utilized SPSS together with GraphPad Prism 5 software for statistical analysis. Student's t-test or chi-square test was employed to estimate differences between 2 groups, whereas one-way analysis of variance (ANOVA) was used to estimate differences between 3 or more groups. The Pearson correlation coefficient was utilized to determine the relation between genes. $P < 0.05$ was significant. All presented data were expressed as means \pm standard error of the mean (SEM).

3. Results

3.1. Circ-JMJD1C and JMJD1C were highly expressed in BC

It has been registered that distinct circRNAs were aberrantly expressed in BC (12). Among them, circJMJD1C possessed the most significant fold changes (12). The UCSC database indicated that circ-JMJD1C (chr10 63,465,896) was formed by the exons of its host gene JMJD1C (Exon 1, chr10: 63,316,601), which implied a potential management of JMJD1C by circ-JMJD1C (data not shown). Additionally, the cyclic structure of circ-JMJD1C was certified as it was only amplified by divergent primers (Figure 1A). Subsequently, the expression of circ-JMJD1C and linear JMJD1C in healthy tissues, para-carcinoma tissues, as well

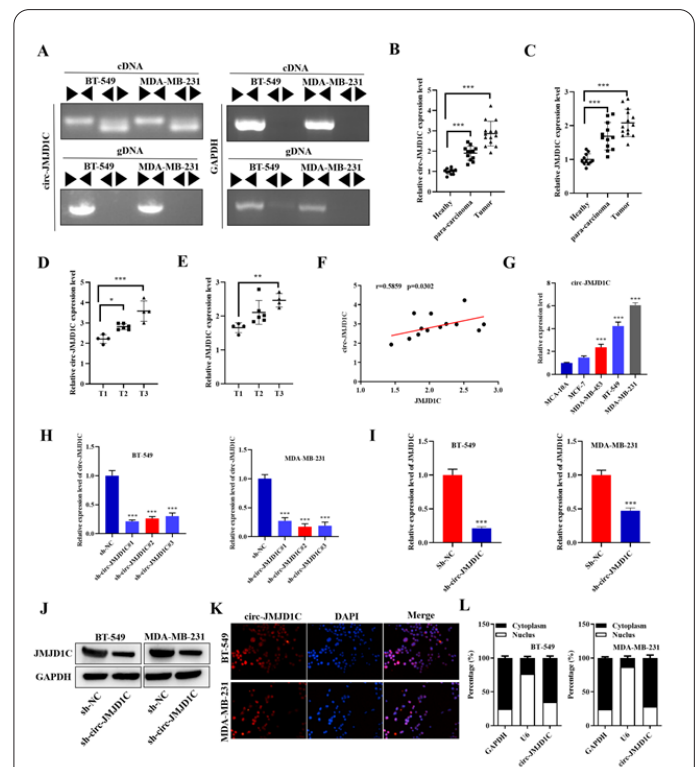


Fig. 1. Circ-JMJD1C and JMJD1C are upregulated in BC. (A) Divergent primer PCR verified the circular structure of circ-JMJD1C. (B-C) qRT-PCR outcomes of circ-JMJD1C and JMJD1C expression in healthy, para-carcinoma, as well as tumor tissues. (D-E) qRT-PCR examined circ-JMJD1C and JMJD1C expression in tumor tissues in T1, T2, as well as T3 stages. (F) Pearson's correlation analysis of circ-JMJD1C and JMJD1C. (G) Circ-JMJD1C expression in BC cells along with MCF-10A from qRT-PCR. (H) qRT-PCR tested the silencing efficiency of circ-JMJD1C in BC cells. (I-J) JMJD1C expression in BC cells after circ-JMJD1C silence from qRT-PCR together with Western blot. (K-L) FISH and subcellular fractionation assays tested the localization of circ-JMJD1C in BC cells. * $P < 0.05$, ** $P < 0.01$, *** $P < 0.001$.

as BC samples were shown as low, middle and high (Figure 1B-C). Notably, the levels of circ-JMJD1C and linear JMJD1C were enhanced accompanied by BC progression (Figure 1D-E). Significantly, in BC tissues, a positive relation between JMJD1C and circ-JMJD1C expression was observed (Figure 1F).

In comparison with normal cells, circ-JMJD1C was highly expressed in BC cells (Figure 1G). Then, circ-JMJD1C was knocked down in two BC cells. As shown in Figure 1H, all shRNAs constructs targeting circ-JMJD1C remarkably reduced circ-JMJD1C expression in both cells. Notably, sh-circ-JMJD1C#1 was chosen for subsequent analysis because of its highest silencing efficiency. Expectedly, circ-JMJD1C inhibition resulted in decreased JMJD1C expression at mRNA along with protein levels (Figure 1I, J). Additionally, the FISH assay indicated the distribution of circ-JMJD1C was mainly in the cytoplasm (Figure 1K), which was also confirmed by qPCR from the fractionated mRNA profile in the cytoplasm and nucleus (Figure 1L).

3.2. Circ-JMJD1C knockdown hindered cell proliferation and promoted breast cancer cell apoptosis

The loss-of-function experiments were arranged to uncover circ-JMJD1C potential in BC. CCK-8 assay demonstrated circ-JMJD1C depletion repressed the viability of two selected BC cells (Figure 2A). Western blot results displayed circ-JMJD1C reduction suppressed Bcl-2 expression whereas elevated of Bax and cleaved caspase-3 levels (Figure 2B). Consistently, the EdU assay manifested BC cell proliferation was reduced upon circ-JMJD1C downregulation (Figure 2C). TUNEL assay demonstrated that BC cell apoptosis was elevated in two selected BC cells after transfection with sh-circ-JMJD1C #1 (Figure 2D). The cell motility declined after circ-JMJD1C knockdown (Figure 2E). Similarly, the transwell assay showed circ-JMJD1C knockdown repressed cell invasion (Figure 2F). Western blot results confirmed the enhanced expression of E-cadherin along with suppression of N-cadherin, MMP2, and MMP9 levels when circ-JMJD1C was knocked down (Figure 2G). Immunofluorescence assay expounded significant decrease of N-cadherin and MMP-2 expression upon circ-JMJD1C downregulation in BC cells (Figure 2H).

3.3. Circ- JMJD1C upregulated JMJD1C expression through sponging miR-182-5p

We discovered that miR-182-5p potentially targets both circ-JMJD1C and JMJD1C (Figure 3A). Then, miR-182-5p was discovered to be low-expressed in all BC cells (Figure 3B). Similarly, we verified that miR-182-5p expression was also drastically reduced in tumor tissues relative to healthy and para-carcinoma specimens (Figure 3C). Besides, miR-182-5p expression was negatively related to circ-JMJD1C expression (Figure 3D). The binding sites of miR-182-5p and circ-JMJD1C or JMJD1C were revealed in Figure 3E. The outcomes of the luciferase reporter assay manifested that overexpressed miR-182-5p could decline the luciferase activity of JMJD1C-WT together with circ-JMJD1C-WT, but did not impact that of JMJD1C-MUT and circ-JMJD1C-MUT (Figure 3F). Besides, it was unraveled that circ-JMJD1C, miR-182-5p, and JMJD1C were abundant in the anti-Ago2 antibody precipitated compounds from RIP assays (Figure 3G). Meanwhile, RNA pull-down experiments suggested that circ-JMJD1C and

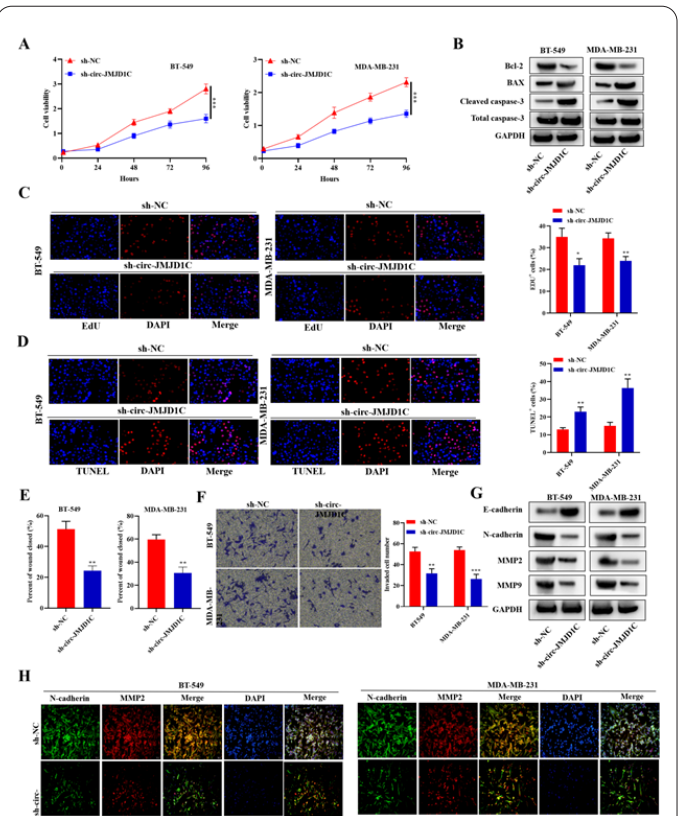


Fig. 2. Silenced circ-JMJD1C reduces BC proliferation and promotes apoptosis. (A) CCK-8 assay detected BC cell proliferation after circ-JMJD1C silence. (B) Levels of apoptosis-linked proteins after circ-JMJD1C silence were assessed by Western blot. (C-D) EdU and TUNEL detected cell proliferation and apoptosis affected by circ-JMJD1C silence in two BC cells. (E-F) BC cells migration and invasion after circ-JMJD1C silence from wound healing assay and Transwell assay. (G) Western blot tested N-cadherin, E-cadherin, MMP2, as well as MMP9 levels after circ-JMJD1C silence. (H) N-cadherin together with MMP-2 levels in two cells after circ-JMJD1C silence were detected via IF assay. * $P < 0.05$, ** $P < 0.01$, *** $P < 0.001$.

JMJD1C were pulled down by miR-182-5p (Figure 3H). MiR-182-5p expression was also negatively related to JMJD1C expression (Figure 3I). Additionally, silenced circ-JMJD1C inhibited JMJD1C expression while promoting the miR-182-5p expression in two BC cells (Figure 3J). Of note, we confirmed that JMJD1C protein expression was inhibited by circ-JMJD1C knockdown and then recovered after cosuppression of miR-182-5p (Figure 3K).

3.4. Circ-JMJD1C/JMJD1C complex epigenetically activates EMT-transcription factor (TF) SOX4

EMT-TF is the core regulator of EMT machinery. The alteration of EMT-TF may promote or reverse the processes of EMT. Therefore, we determined the expression of EMT-TF in breast cancer. As shown in Figure 4A, we found that SOX4 expression was significantly increased in breast cancer patients, while TWIST1 and ZEB1 expression were significantly downregulated. Moreover, we determined the expression of SOX4, TWIST1 and ZEB1. We found that the mRNA expression of SOX4, TWIST1 and ZEB1 was significantly upregulated by overexpressed circ-JMJD1C (Figure 4B), while decreased by circ-JMJD1C knockdown. Moreover, SOX4 expression was positively correlated with that of JMJD1C (Figure 4C). High expression of SOX4 predicted poor survival rates in

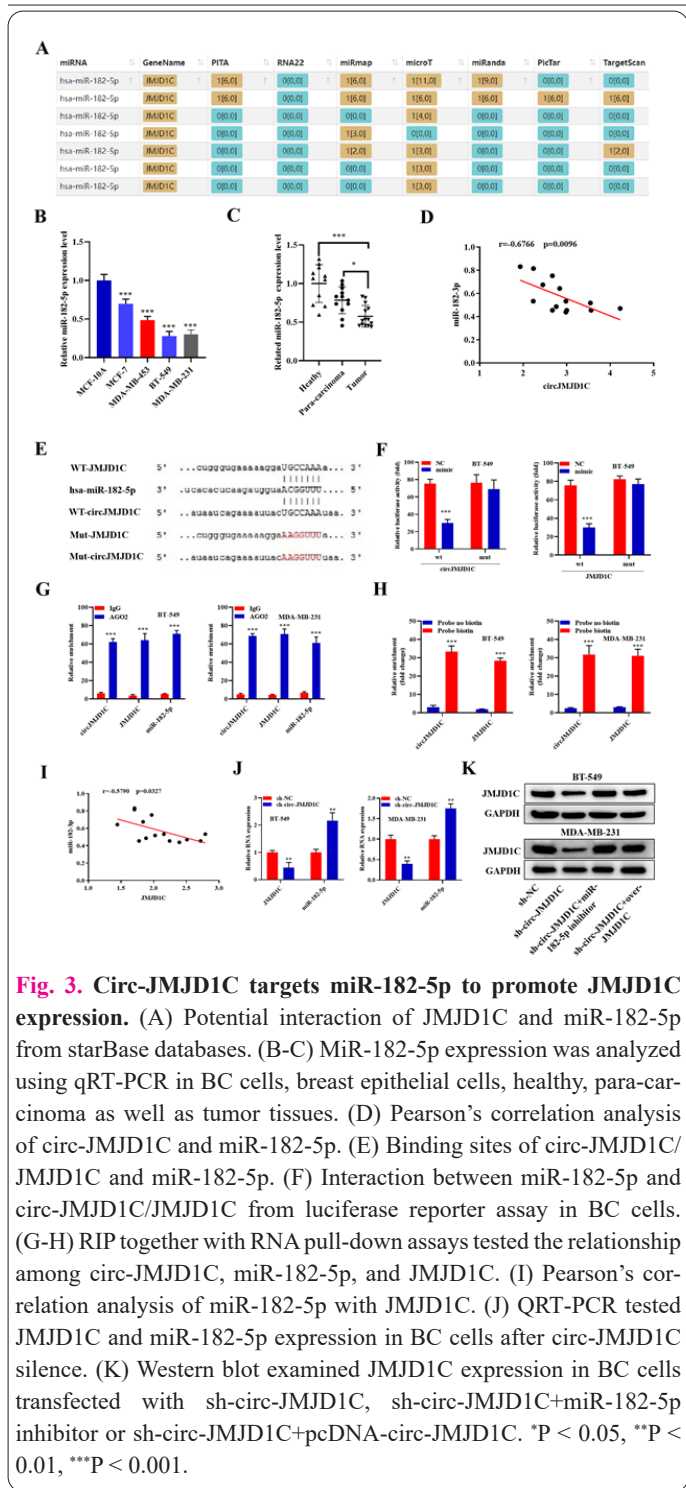


Fig. 3. Circ-JMJD1C targets miR-182-5p to promote JMJD1C expression. (A) Potential interaction of JMJD1C and miR-182-5p from starBase databases. (B-C) MiR-182-5p expression was analyzed using qRT-PCR in BC cells, breast epithelial cells, healthy, para-carcinoma as well as tumor tissues. (D) Pearson's correlation analysis of circ-JMJD1C and miR-182-5p. (E) Binding sites of circ-JMJD1C/JMJD1C and miR-182-5p. (F) Interaction between miR-182-5p and circ-JMJD1C/JMJD1C from luciferase reporter assay in BC cells. (G-H) RIP together with RNA pull-down assays tested the relationship among circ-JMJD1C, miR-182-5p, and JMJD1C. (I) Pearson's correlation analysis of miR-182-5p with JMJD1C. (J) QRT-PCR tested JMJD1C and miR-182-5p expression in BC cells after circ-JMJD1C silence. (K) Western blot examined JMJD1C expression in BC cells transfected with sh-circ-JMJD1C, sh-circ-JMJD1C+miR-182-5p inhibitor or sh-circ-JMJD1C+pcDNA-circ-JMJD1C. *P < 0.05, **P < 0.01, ***P < 0.001.

3.5. Knockdown of circ-JMJD1C impeded BC tumor growth in vivo

Animals were injected with circ-JMJD1C-silenced BC cells. We found the tumors were shrunken and distinctly more diminutive due to circ-JMJD1C decrease (Figure

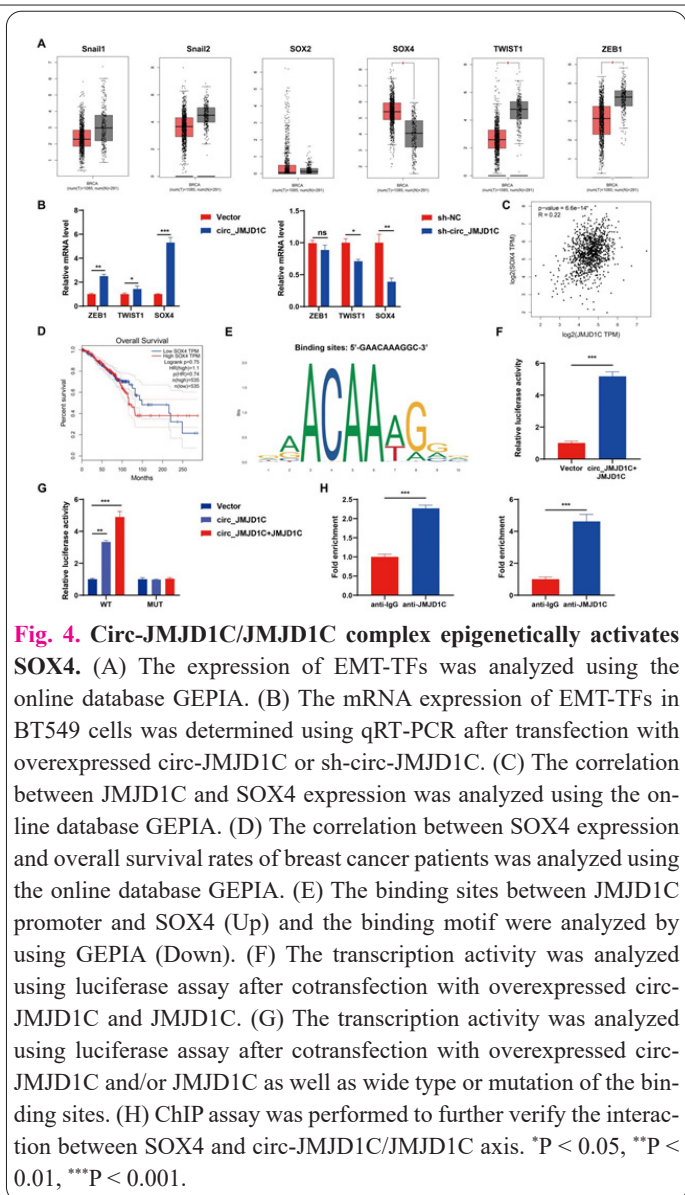


Fig. 4. Circ-JMJD1C/JMJD1C complex epigenetically activates SOX4. (A) The expression of EMT-TFs was analyzed using the online database GEPIA. (B) The mRNA expression of EMT-TFs in BT549 cells was determined using qRT-PCR after transfection with overexpressed circ-JMJD1C or sh-circ-JMJD1C. (C) The correlation between JMJD1C and SOX4 expression was analyzed using the online database GEPIA. (D) The correlation between SOX4 expression and overall survival rates of breast cancer patients was analyzed using the online database GEPIA. (E) The binding sites between JMJD1C promoter and SOX4 (Up) and the binding motif were analyzed by using GEPIA (Down). (F) The transcription activity was analyzed using luciferase assay after cotransfection with overexpressed circ-JMJD1C and JMJD1C. (G) The transcription activity was analyzed using luciferase assay after cotransfection with overexpressed circ-JMJD1C and/or JMJD1C as well as wide type or mutation of the binding sites. (H) ChIP assay was performed to further verify the interaction between SOX4 and circ-JMJD1C/JMJD1C axis. *P < 0.05, **P < 0.01, ***P < 0.001.

4. Discussion

In this study, circRNA_104348 was overexpressed in breast cancer patients and cells. Moreover, high levels of circRNA_104348 were associated with tumorigenesis and advanced stages. Interestingly, circRNA_104348 knockdown suppressed the proliferation and EMT of breast cancer cells, while promoting tumor cell apoptosis. Moreover, circRNA_104348 sponged miR-182-5p to upregulate its cognate gene JMJD1C, the knockdown of which promotes suppressed the aggressiveness of breast cancer cells. Therefore, circRNA_104348/miR-182-5p/JMJD1C may be a potential target for breast cancer.

Non-coding RNAs comprise broad types of RNAs,

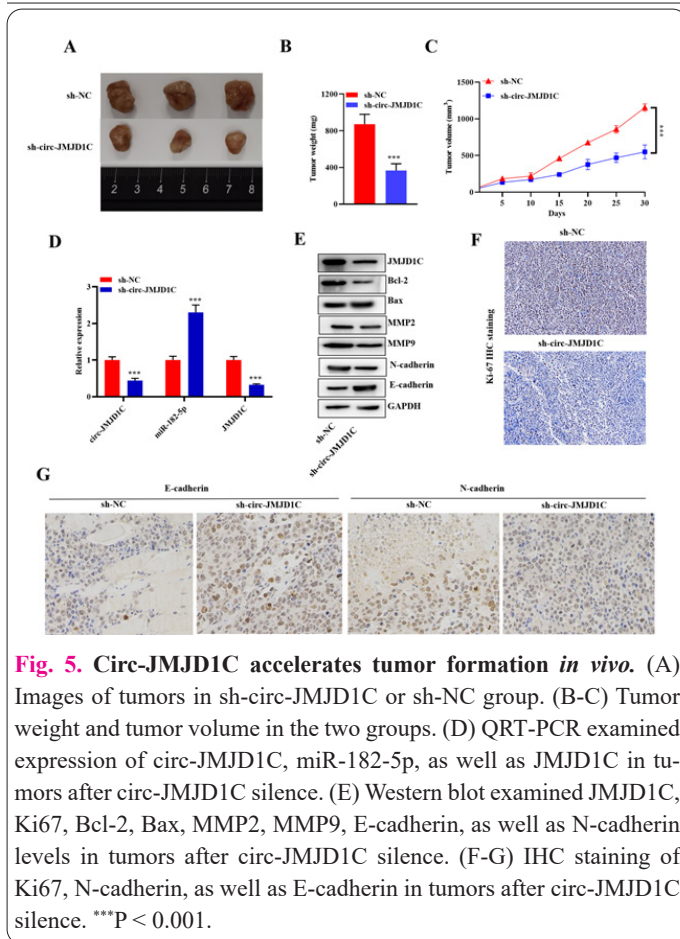


Fig. 5. Circ-JMJD1C accelerates tumor formation *in vivo*. (A) Images of tumors in sh-circ-JMJD1C or sh-NC group. (B-C) Tumor weight and tumor volume in the two groups. (D) QRT-PCR examined expression of circ-JMJD1C, miR-182-5p, as well as JMJD1C in tumors after circ-JMJD1C silence. (E) Western blot examined JMJD1C, Ki67, Bcl-2, Bax, MMP2, MMP9, E-cadherin, as well as N-cadherin levels in tumors after circ-JMJD1C silence. (F-G) IHC staining of Ki67, N-cadherin, as well as E-cadherin in tumors after circ-JMJD1C silence. *** $P < 0.001$.

among which circRNA has a regulatory role in the biological process of cancer [15, 16]. CircRNAs are distinctly involved in the development of cancer. For example, hsa_circRNA_104348 facilitates hepatocellular carcinoma progression via the Wnt/ β -catenin pathway [17]. Overexpression circRNA_102231 accelerates gastric cancer progression [18]. CircRNA_100876 expedites proliferation as well as metastasis of colorectal cancer [19]. Nevertheless, the documents on circRNAs in cancers remain inadequate. Circ_0006743 (circ_JMJD1C) has been shown to be aberrantly upregulated in BC [12], but no functional analysis has been conducted to explore its underlying mechanism and role in BC progression. In this work, circ_JMJD1C significantly increased breast cancer cells and tissues. High expression of circ_JMJD1C predicted poor clinical outcomes. Interestingly, circ_JMJD1C knockdown of circ_JMJD1C suppressed the proliferation and EMT of breast cancer cells as well as promoted the apoptosis of tumor cells. Therefore, circ_JMJD1C may function as onco-circRNA in breast cancer. Inhibition of circ_JMJD1C with specific shRNAs may be a promising strategy for breast cancer.

Increasing evidences demonstrate that circRNAs participate in the regulation of biological processes via sponging miRNAs. We, therefore, explored the role of circ-JMJD1C in the ceRNA model. Bioinformatics analysis showed that miR-182-5p could combine with circ-JMJD1C. Accumulating literatures has implied the tumor-suppressing potential of miR-182-5p. For instance, overexpression of miR-182-5p inhibits the proliferation migration and invasion of colon cancer [20]. Moreover, miR-182-5p suppresses tumor growth and metastasis of colorectal cancer (CRC) [21]. These findings suggest that miR-182-5p may function as an anti-tumor miRNA. However, the roles

of miR-182-5p in tumorigenesis are contradictory. High expression of miR-182-5p predicts advanced tumor-node-metastasis (TNM) stages and lymph node metastasis in patients with non-small cell lung cancer [22]. miR-182-5p promotes tumor cell growth in liver cancer [23]. miR-182-5p accelerates radioresistance in nasopharyngeal carcinoma [24]. These findings dictate that miR-182-5p may also function as an onco-miRNA. Therefore, identifying the exact roles of miR-182-5p in breast cancer is of vital importance. In our study, miR-182-5p was downregulated in breast cancer patients and cells. However, miR-182-5p deficiency promoted the proliferation and EMT of breast cancer cells, suggesting that miR-182-5p may function as an anti-tumor miRNA in breast cancer.

circRNAs function as ceRNA to regulate gene expression via sponging miRNAs. For instance, circSEPT9/miR-637/LIF axis promotes the carcinogenesis and development of triple-negative breast cancer [25]. circRNF20 drives the Warburg effect and tumorigenesis in breast cancer through regulating miR-487a/HIF-1 α /HK2 [11]. In this study, circ-JMJD1C-mediated upregulation of JMJD1C via binding to miR-182-5p, thereby affecting the cellular activity of BC. JMJD and its isoforms were explicitly observed to be promoted and engaged in the development of BC [13]. In this study, JMJD1C was overexpressed in breast cancer cells and tissues. circ-JMJD1C expression was positively correlated with that of JMJD1C in breast cancer tissues. Moreover, circ-JMJD1C was majorly localized in the cytoplasm of BC cells, implying that circ-JMJD1C may participate in the ceRNA network by modulating JMJD1C.

Epithelial-mesenchymal transition (EMT) is characterized by the degradation of epithelial functions and the acquisition of mesenchymal features [26], which is accompanied by the downregulation of E-cadherin and upregulation of N-cadherin, Vimentin, Fibronectin, etc. EMT is associated with tumor initiation, growth, immunosurveillance, and metastasis [27-29]. Activated EMT signaling promotes the metastasis and chemoresistance of breast cancer [30, 31]. EMT-inducing transcription factors (EMT-TFs) play a key role in tumorigenesis. EMT-TFs accelerate the processes of EMT via activating mesenchymal genes and inhibiting epithelial genes [32]. The nuclear interaction of EMT-TFs with larger protein complexes in epigenetic reprogramming during the pathogenesis of breast cancer has attracted increasing attention in recent years. For instance, high levels of ZEB1,2 drive epithelial-mesenchymal plasticity (EMP) in estrogen receptor-positive breast cancer dormancy [33]. Nuclear localization of TWIST1 induces breast tumor invasion and metastasis *in vivo* [34]. In this study, we found that SOX4 was overexpressed in breast cancer. Moreover, high expression of SOX4 was associated with poor survival of breast cancer patients. circ-JMJD1C epigenetically upregulated SOX4, which induced the activation of mesenchymal genes and promoted the EMT of breast cancer cells.

In conclusion, the present study demonstrated that circ-JMJD1C, derived from the host gene JMJD1C, induces BC oncogenesis from miR-182-5p-JMJD1C-SOX4 axis. Our results suggested a novel therapeutic approach for BC patients.

Informed consent

The authors report no conflict of interest.

Availability of data and material

We declared that we embedded all data in the manuscript.

Authors' contributions

XR conducted the experiments and wrote the paper; LH, ZL, YS and MY analyzed and organized the data; CH conceived, designed the study and revised the manuscript.

Funding

None.

Acknowledgements

We thanked Zigong First People's Hospital for approval of our study.

References

- Torre LA, Bray F, Siegel RL, Ferlay J, Lortet-Tieulent J, Jemal A (2015) Global cancer statistics, 2012. *CA Cancer J Clin* 65 (2): 87-108. doi: 10.3322/caac.21262
- Fahad Ullah M (2019) Breast Cancer: Current Perspectives on the Disease Status. *Adv Exp Med Biol* 1152: 51-64. doi: 10.1007/978-3-030-20301-6_4
- Mahvi DA, Liu R, Grinstaff MW, Colson YL, Raut CP (2018) Local Cancer Recurrence: The Realities, Challenges, and Opportunities for New Therapies. *CA Cancer J Clin* 68 (6): 488-505. doi: 10.3322/caac.21498
- DeSantis C, Ma J, Bryan L, Jemal A (2014) Breast cancer statistics, 2013. *CA Cancer J Clin* 64 (1): 52-62. doi: 10.3322/caac.21203
- Danan M, Schwartz S, Edelheit S, Sorek R (2012) Transcriptome-wide discovery of circular RNAs in Archaea. *Nucleic Acids Res* 40 (7): 3131-3142. doi: 10.1093/nar/gkr1009
- Jeck WR, Sharpless NE (2014) Detecting and characterizing circular RNAs. *Nat Biotechnol* 32 (5): 453-461. doi: 10.1038/nbt.2890
- Croce CM (2016) Genetics: Are circRNAs involved in cancer pathogenesis? *Nat Rev Clin Oncol* 13 (11): 658. doi: 10.1038/nrclinonc.2016.113
- Smid M, Wilting SM, Uhr K, Rodriguez-Gonzalez FG, de Weerd V, Prager-Van der Smissen WJC, van der Vlugt-Daane M, van Galen A, Nik-Zainal S, Butler A, Martin S, Davies HR, Staaf J, van de Vijver MJ, Richardson AL, MacGrogan G, Salgado R, van den Eynden G, Purdie CA, Thompson AM, Caldas C, Span PN, Sweep F, Simpson PT, Lakhani SR, Van Laere S, Desmedt C, Paradiso A, Eyfjord J, Broeks A, Vincent-Salomon A, Futreal AP, Knappskog S, King T, Viari A, Borresen-Dale AL, Stunnenberg HG, Stratton M, Foekens JA, Sieuwerts AM, Martens JWM (2019) The circular RNome of primary breast cancer. *Genome Res* 29 (3): 356-366. doi: 10.1101/gr.238121.118
- Sang Y, Chen B, Song X, Li Y, Liang Y, Han D, Zhang N, Zhang H, Liu Y, Chen T, Li C, Wang L, Zhao W, Yang Q (2019) circRNA_0025202 Regulates Tamoxifen Sensitivity and Tumor Progression via Regulating the miR-182-5p/FOXO3a Axis in Breast Cancer. *Mol Ther* 27 (9): 1638-1652. doi: 10.1016/j.ymthe.2019.05.011
- Liang G, Ling Y, Mehrpour M, Saw PE, Liu Z, Tan W, Tian Z, Zhong W, Lin W, Luo Q, Lin Q, Li Q, Zhou Y, Hamai A, Codogno P, Li J, Song E, Gong C (2020) Autophagy-associated circRNA circCDYL augments autophagy and promotes breast cancer progression. *Mol Cancer* 19 (1): 65. doi: 10.1186/s12943-020-01152-2
- Cao L, Wang M, Dong Y, Xu B, Chen J, Ding Y, Qiu S, Li L, Karamfilova Zaharieva E, Zhou X, Xu Y (2020) Circular RNA circRNF20 promotes breast cancer tumorigenesis and Warburg effect through miR-487a/HIF-1alpha/HK2. *Cell Death Dis* 11 (2): 145. doi: 10.1038/s41419-020-2336-0
- Rao A, Arvinden VR, Ramasamy D, Patel K, Meenakumari B, Ramanathan P, Sundersingh S, Sridevi V, Rajkumar T, Herceg Z, Gowda H, Mani S (2021) Identification of novel dysregulated circular RNAs in early-stage breast cancer. *J Cell Mol Med* 25 (8): 3912-3921. doi: 10.1111/jcmm.16324
- Sui Y, Gu R, Janknecht R (2021) Crucial Functions of the JMJD1/KDM3 Epigenetic Regulators in Cancer. *Mol Cancer Res* 19 (1): 3-13. doi: 10.1158/1541-7786.MCR-20-0404
- Pan G, Mao A, Liu J, Lu J, Ding J, Liu W (2020) Circular RNA hsa_circ_0061825 (circ-TFF1) contributes to breast cancer progression through targeting miR-326/TFF1 signalling. *Cell Prolif* 53 (2): e12720. doi: 10.1111/cpr.12720
- Memczak S, Jens M, Elefsinioti A, Torti F, Krueger J, Rybak A, Maier L, Mackowiak SD, Gregersen LH, Munschauer M, Loewer A, Ziebold U, Landthaler M, Kocks C, le Noble F, Rajewsky N (2013) Circular RNAs are a large class of animal RNAs with regulatory potency. *Nature* 495 (7441): 333-338. doi: 10.1038/nature11928
- Sun HD, Xu ZP, Sun ZQ, Zhu B, Wang Q, Zhou J, Jin H, Zhao A, Tang WW, Cao XF (2018) Down-regulation of circPVRL3 promotes the proliferation and migration of gastric cancer cells. *Sci Rep* 8 (1): 10111. doi: 10.1038/s41598-018-27837-9
- Huang G, Liang M, Liu H, Huang J, Li P, Wang C, Zhang Y, Lin Y, Jiang X (2020) CircRNA hsa_circRNA_104348 promotes hepatocellular carcinoma progression through modulating miR-187-3p/RTKN2 axis and activating Wnt/beta-catenin pathway. *Cell Death Dis* 11 (12): 1065. doi: 10.1038/s41419-020-03276-1
- Yuan G, Ding W, Sun B, Zhu L, Gao Y, Chen L (2021) Upregulated circRNA_102231 promotes gastric cancer progression and its clinical significance. *Bioengineered* 12 (1): 4936-4945. doi: 10.1080/21655979.2021.1960769
- Zhang J, Wang H, Wu K, Zhan F, Zeng H (2020) Dysregulated circRNA_100876 contributes to proliferation and metastasis of colorectal cancer by targeting microRNA-516b (miR-516b). *Cancer Biol Ther* 21 (8): 733-740. doi: 10.1080/15384047.2020.1776075
- Yan S, Wang H, Chen X, Liang C, Shang W, Wang L, Li J, Xu D (2020) MiR-182-5p inhibits colon cancer tumorigenesis, angiogenesis, and lymphangiogenesis by directly downregulating VEGF-C. *Cancer Lett* 488: 18-26. doi: 10.1016/j.canlet.2020.04.021
- Jin Y, Zhang ZL, Huang Y, Zhang KN, Xiong B (2019) MiR-182-5p inhibited proliferation and metastasis of colorectal cancer by targeting MTDH. *Eur Rev Med Pharmacol Sci* 23 (4): 1494-1501. doi: 10.26355/eurrev_201902_17107
- Gao L, Yan SB, Yang J, Kong JL, Shi K, Ma FC, Huang LZ, Luo J, Yin SY, He RQ, Hu XH, Chen G (2020) MiR-182-5p and its target HOXA9 in non-small cell lung cancer: a clinical and in-silico exploration with the combination of RT-qPCR, miRNA-seq and miRNA-chip. *BMC Med Genomics* 13 (1): 3. doi: 10.1186/s12920-019-0648-7
- Zheng J, Wu D, Wang L, Qu F, Cheng D, Liu X (2021) miR-182-5p Regulates Cell Growth of Liver Cancer via Targeting RCAN1. *Gastroenterol Res Pract* 2021: 6691305. doi: 10.1155/2021/6691305
- He W, Jin H, Liu Q, Sun Q (2021) miR-182-5p contributes to radioresistance in nasopharyngeal carcinoma by regulating BNIP3 expression. *Mol Med Rep* 23 (2). doi: 10.3892/mmr.2020.11769
- Zheng X, Huang M, Xing L, Yang R, Wang X, Jiang R, Zhang L, Chen J (2020) The circRNA circSEPT9 mediated by E2F1 and EIF4A3 facilitates the carcinogenesis and development of triple-negative breast cancer. *Mol Cancer* 19 (1): 73. doi: 10.1186/s12943-020-01183-9

26. Dongre A, Weinberg RA (2019) New insights into the mechanisms of epithelial-mesenchymal transition and implications for cancer. *Nat Rev Mol Cell Biol* 20 (2): 69-84. doi: 10.1038/s41580-018-0080-4
27. Mittal V (2018) Epithelial Mesenchymal Transition in Tumor Metastasis. *Annu Rev Pathol* 13: 395-412. doi: 10.1146/annurev-pathol-020117-043854
28. Chen HT, Liu H, Mao MJ, Tan Y, Mo XQ, Meng XJ, Cao MT, Zhong CY, Liu Y, Shan H, Jiang GM (2019) Crosstalk between autophagy and epithelial-mesenchymal transition and its application in cancer therapy. *Mol Cancer* 18 (1): 101. doi: 10.1186/s12943-019-1030-2
29. Taki M, Abiko K, Ukita M, Murakami R, Yamanoi K, Yamaguchi K, Hamanishi J, Baba T, Matsumura N, Mandai M (2021) Tumor Immune Microenvironment during Epithelial-Mesenchymal Transition. *Clin Cancer Res* 27 (17): 4669-4679. doi: 10.1158/1078-0432.CCR-20-4459
30. Grasset EM, Dunworth M, Sharma G, Loth M, Tandurella J, Cimino-Mathews A, Gentz M, Bracht S, Haynes M, Fertig EJ, Ewald AJ (2022) Triple-negative breast cancer metastasis involves complex epithelial-mesenchymal transition dynamics and requires vimentin. *Sci Transl Med* 14 (656): eabn7571. doi: 10.1126/scitranslmed.abn7571
31. Gooding AJ, Schiemann WP (2020) Epithelial-Mesenchymal Transition Programs and Cancer Stem Cell Phenotypes: Mediators of Breast Cancer Therapy Resistance. *Mol Cancer Res* 18 (9): 1257-1270. doi: 10.1158/1541-7786.MCR-20-0067
32. Skrypek N, Goossens S, De Smedt E, Vandamme N, Berx G (2017) Epithelial-to-Mesenchymal Transition: Epigenetic Reprogramming Driving Cellular Plasticity. *Trends Genet* 33 (12): 943-959. doi: 10.1016/j.tig.2017.08.004
33. Subbalakshmi AR, Sahoo S, McMullen I, Saxena AN, Venugopal SK, Somarelli JA, Jolly MK (2021) KLF4 Induces Mesenchymal-Epithelial Transition (MET) by Suppressing Multiple EMT-Inducing Transcription Factors. *Cancers (Basel)* 13 (20). doi: 10.3390/cancers13205135
34. Fattet L, Jung HY, Matsumoto MW, Aubol BE, Kumar A, Adams JA, Chen AC, Sah RL, Engler AJ, Pasquale EB, Yang J (2020) Matrix Rigidity Controls Epithelial-Mesenchymal Plasticity and Tumor Metastasis via a Mechanoresponsive EPHA2/LYN Complex. *Dev Cell* 54 (3): 302-316 e307. doi: 10.1016/j.devcel.2020.05.031